Atkin, C.J. (2001). New aerodynamic approaches to suction system design. Notes on Numerical Fluid Mechanics, 76(3), pp. 55-63. doi: 10.1007/978-3-540-45359-8_7

New Aerodynamic Approach to Suction System Design

Chris Atkin, Aerodynamics Department,
Küchemann Building, DERA Farnborough, Hants, GU14 0LX, UK.

Summary

A new approach to the aerodynamic design of Hybrid Laminar Flow Control suction systems is presented. The definition of suction chamber layout and pressures has been closely coupled with the boundary layer and stability analysis methodology to provide a numerical tool to help in the design of a suction system. The new approach also provides a direct link between the cost functions of suction system mass and power with the aerodynamic drag benefit, yielding a more streamlined design procedure. Practical constraints appear at an early stage in the process rather than late in the day after much effort has been expended. To demonstrate the power of the technique, the advantages and penalties associated with two different chamber layouts are discussed. Further research is required into the control of crossflow instability and the over-suction phenomenon before the method can be fully exploited.

Introduction

The past two decades have seen a revival of interest in Hybrid Laminar Flow Control (HLFC) for the reduction of drag/fuel burn of transport aircraft, largely because of increased concerns about the environmental impact of commercial air traffic at high altitude. As confidence has grown that the technical problems do, in fact, have solutions, the question of commercial viability has arisen. Recent progress means that this issue can now be addressed with some confidence. Another important issue is that the introduction of a new aircraft boasting a new technology such as HLFC may be a risk too far for the civil aerospace industry. One of the issues tackled by the EU 4th Framework HYLTEC project is the possibility of retro-fitting HLFC technology to a mature aircraft product. The assessment of the potential of a retrofit solution is being undertaken within task 2 of the HYLTEC project. The Airbus Industrie A310 was selected as the baseline aircraft for this task.

The aerodynamic design of HLFC systems focuses on two issues: where to apply suction, and how much suction to apply. In earlier HLFC programmes, the suction region was limited to the area forward of the front spar, so as to minimise impact on wing structure and fuel volume, and suction rates had to be flexible to aid in the learning process. With the maturing of HLFC technology, the answers and indeed the questions have become more sophisticated. The concern is now directly with the design of the plenum chambers: where to place them, how many to have and how large, and what the chamber pressures should be. The goal is not necessarily to maximise laminar flow, but to optimise *performance* including aerodynamic, system and structural penalties as well as simple profile drag reduction.

The objective of the present work is to re-organise the aerodynamic design process to reflect modern design issues and to facilitate the integration of aerodynamics into a multi-disciplinary design procedure. For brevity, the results shown in this paper focus on one of the HYLTEC design points, that of the A310 wing at a Mach number of 0.8, a mean chord Reynolds number of 30 million, and a sectional lift coefficient towards the upper end of the operational range. The form of the sectional pressure distribution for this case is shown in Figure 1(a). Clearly,

Notes on Numerical Fluid Mechanics, Vol. 76, P Thiede (ed.), Springer, 2001.
(Proceedings of the CEAS/DragNet European Drag Reduction Conference, Potsdam, June 2000.)

the aircraft designer would cover a range of operating points, but the application of the approach to this single case will serve to demonstrate the basic principles.

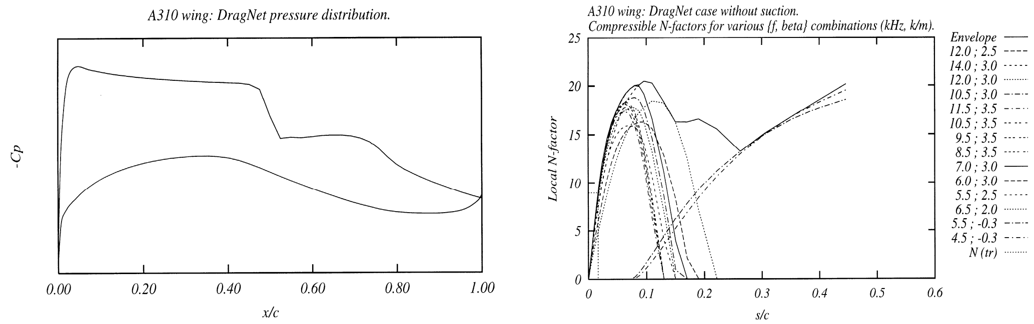

Figure 1 (a) Pressure distribution for A310 test case and (b) corresponding N-factors (no suction).

The basic tools of aerodynamic HLFC analysis are the swept-tapered laminar boundary layer and the e^N transition prediction methods. An example of the output from these tools is illustrated in Figure 1(b). The amplitude of all boundary layer instabilities of crossflow (CF) or Tollmien-Schlichting (TS) type is expressed in terms of N-factors, one curve for each possible mode of instability. Figure 1(b) shows a selection of most-amplified modes and the envelope-of-envelopes curve showing the variation of maximum N-factor with chordwise position. The DERA stability method [1] uses the constant-spanwise-wavenumber integration strategy and the envelope-of-envelopes analysis; no filtering of modes takes place and a single N-factor criterion is applied for all modes. Of course there is nothing to stop the automatic technique which follows from being coupled with any other e^N strategy.

For this single N-factor strategy a correlated value of N = 9 at transition can be inferred from the literature [2] (coincidental, perhaps, with the classically quoted value for 2D flows). Applying this criterion, it can be seen that, for this test case, transition without HLFC would be expected to occur at about 2% chord *s/c*. The N-factors exhibit a peak near the leading edge where crossflow instability causes transition in the absence of any turbulent contamination of the leading edge flow. The crossflow instabilities are subsequently damped downstream of the suction peak where Tollmien-Schlichting instabilities take over. No N-factors are seen beyond 45% chord where the shock wave would cause laminar separation.

Review of classical aerodynamic HLFC system design

Laminar flow control originated with theoretical aerodynamics and the flow through a real porous wing surface is still usually modelled with an analytical velocity distribution. This distribution observes certain practical constraints, for example that suction be applied only on the wing upper surface and that the suction system cannot extend into the main wing box aft of 20% chord. Since it is observed that suction is more efficient towards the leading edge, where instability first occurs, the distribution is trapezoidal in shape. Furthermore, by constraining the shape the suction distribution can be characterised by a single parameter (e.g. maximum suction velocity). This simplifies the optimisation of such a suction system.

The crudest approach is to apply sufficient suction to remove all instability over the porous region, thereby delaying the whole transition process by at least the length of the suction region, or in the present case pushing transition as far aft as 35% chord, Figure 2(a). The corresponding velocity distribution, Figure 2(b), is expressed as notional local hole velocities. A more sophisticated approach is to vary the suction rate and to examine the movement of transition: as the mean suction velocity increases, the transition mechanism changes suddenly from CF-induced to TS-induced, much further aft on the wing. This leads to a recommended suction rate which is just sufficient to push transition aft to the mid-chord region. Figure 3 shows how, with a transition N-factor of 9, this can be achieved with much less suction (about half) than that required for the complete stabilisation of CF modes.

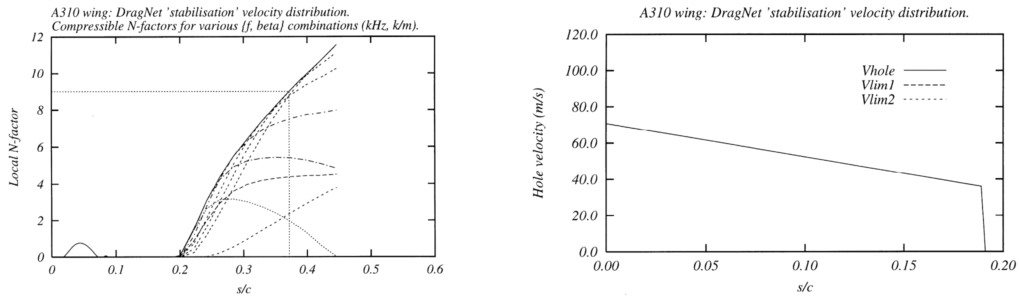

Figure 2 (a) Complete stabilisation of CF modes and (b) corresponding velocity distribution.

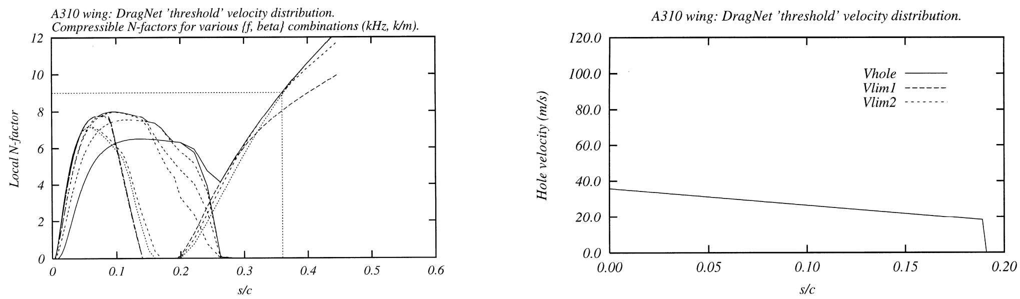

Figure 3 (a) 'Avoidance' of CF transition and (b) corresponding velocity distribution.

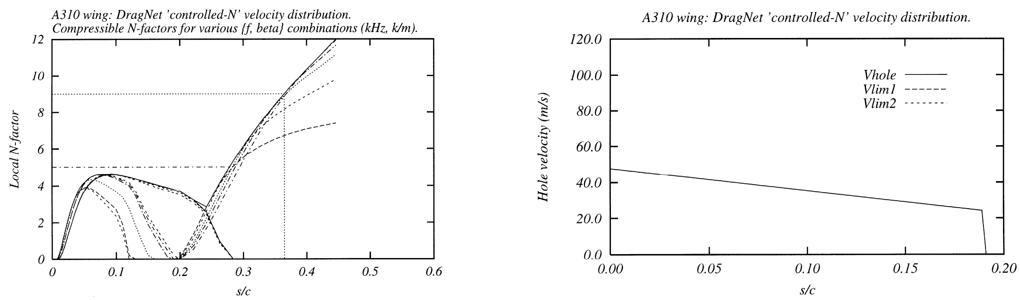

Figure 4 (a) N-factor control of CF modes and (b) corresponding velocity distribution.

There are risks with this approach: the e^N method bundles all the non-linear effects known to occur in the latter stages of transition into the critical N-factor. However, the threshold design approach allows instability growth right up to non-linear amplitudes some way ahead of the predicted transition location. In practice the flow is likely to be dominated by non-linear effects from that point onward, invalidating the subsequent predictions of the linear model. A third approach has therefore been proposed where the crossflow N-factor region is controlled so that instabilities are contained within the boundaries of linear behaviour. For example, limiting the N-factor to be 5 or lower represents a factor of 50 between the control amplitude and the 'critical' amplitude. This approach is shown in Figure 4. The hole velocities are about 40% higher than for the threshold approach but 30% lower than for complete stabilisation. The question remains as to what is an acceptable N-factor margin to avoid non-linear effects.

Practical realisation of surface suction

Wall transpiration is actually implemented by sucking air through a laser-drilled skin. The velocity through each drilled hole is determined by the pressure drop across the skin, the geometry of the hole and the flow conditions at the mouth of the hole. The exact relationship used in this work was derived by ONERA [3]. We average out the separate hole flows into a mean transpiration velocity using the hole area ratio but the exact validity of this averaging has never been thoroughly investigated. We know that high individual hole velocities generate secondary flows in the boundary of a vortical nature which cannot be modelled by the linear stability tools used for HLFC design. These secondary flows are avoided by using over-suction criteria. Two recent experimental investigations into over-suction were carried out by Reneaux & Blanchard (R&B) [4] at ONERA, who derived the expression

$$\frac{V_{h,crit}}{U_e} = \frac{2}{\pi R_{\delta^*}}\left(\frac{\delta^*}{\delta}\right)\left[P_0^2\left(\frac{\phi}{\delta^*}\right)^{-1} - 2P_0P_1 + P_1^2\left(\frac{\phi}{\delta^*}\right)\right], \tag{1}$$

and by Ellis & Poll (E&P) [3] at Manchester University, whose results can be expressed by

$$\frac{V_{h,crit}}{U_e} \sim \left(\frac{\phi}{\delta^*}\right)^{-7/4}\left(\frac{L}{D}\right)^{-1/4}. \tag{2}$$

V_h and U_e are the hole and edge flow velocities respectively, ϕ and δ^* are the hole diameter and boundary layer displacement thickness, R_{δ^*} is the Reynolds number based on δ^*. L and D are the suction length and hole spacing respectively: L/D represents the number of rows of suction holes The P_n terms are constants obtained from a line-fit. One difficulty in reconciling the results of E&P with those of R&B is the lack of an explicit dependence on R_{δ^*} in equation (2) compared with equation (1). Another obvious difference is the functional dependence of V_h on ϕ/δ^*, arising principally from the linear and logarithmic figures used by the two research groups, although it may be connected with the differing R_{δ^*} dependence. It does, however, appear that a power law might fit the data of R&B better than the linear relationship, especially for $\phi/\delta^* < 1$ which would be typical of flight conditions. The effect of suction length, observed by both research groups, is only quantified by E&P. The differences between the two investigations can be resolved only by further experiments which should also cover the influence of the local boundary layer profile shape, including three-dimensionality. Concluding this too brief review on over-suction, a composite relation, more general than equations (1) and (2) but calibrated against them, was used in the current work:

$$\frac{V_{h,crit}}{U_e} \sim \frac{1}{R_{\delta^*}}\left(\frac{\phi}{\delta^*}\right)^{-7/4}\left(\frac{L}{D}\right)^{-1/4} \tag{3}$$

Practical suction distributions

The simplest approach to chamber layout is to try to match the analytical transpiration velocity distributions derived using the aerodynamic analysis described above. This is clearly an easier job than tackling chamber layout *ab initio* because the aerodynamic parametric study then involves only one variable, the average suction rate. Figure 5(a) illustrates such a 6-chamber layout designed to reproduce the velocity distribution of Figure 4(b): the actual resultant distribution is shown in Figure 5(b). These figures also show the over-suction limits *Plim1/Vlim1* corresponding to equation (3) above, and *Plim2/Vlim2* corresponding to a hole Mach number limit of 0.5. The first limit only seems to be significant near the leading edge where the boundary layer is at its thinnest.

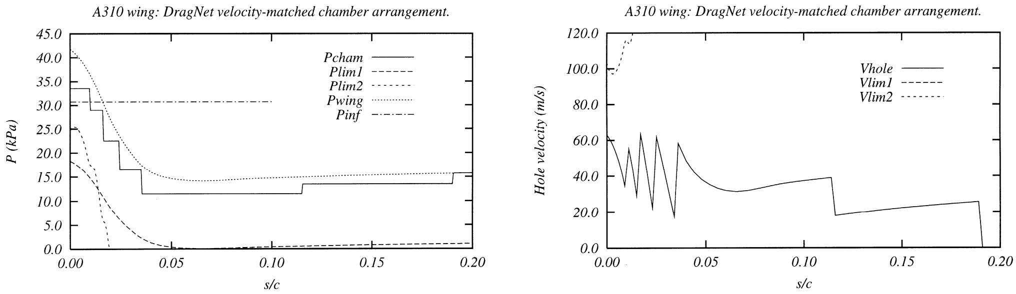

Figure 5 (a) Chamber layout and (b) corresponding velocity distribution devised to match Figure 4.

The resultant velocity distribution shown in Figure 5(b) is very jagged near the leading edge due to the finite chamber lengths and the external pressure gradient. Although it is recognisably close to the distribution in Figure 4(b), the aerodynamic constraints met by the analytical suction distribution are not reliably met by the chamber design. In this case the N-factors exceed the suction-zone limit by about 20%. However the approach can always be improved in this respect by using a larger number of smaller chambers. But is this is actually necessary?

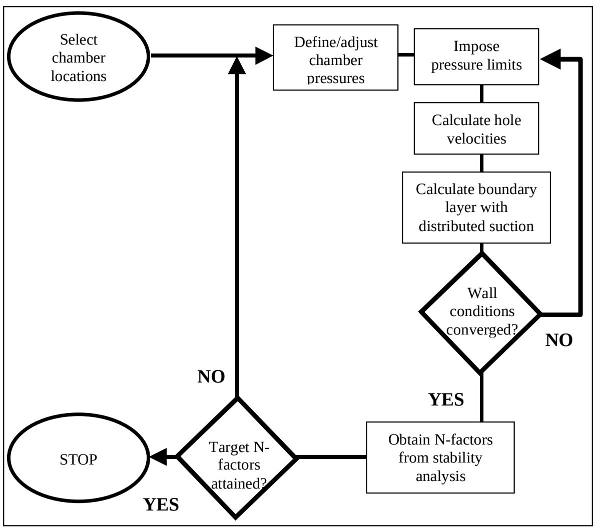

Figure 6: flow diagram of integrated chamber layout and aerodynamic analysis process.

New approach

The new approach simply involves the integration of the various steps described above, with the important difference that the chamber layout is proposed first and used directly to generate input for the boundary layer and stability analysis: no analytical velocity distributions are required. The N-factors from the stability analysis are then used to control the chamber pressures until the aerodynamic laminar flow constraints are achieved. A schematic of the process is shown in Figure 6. The process starts with the specification of chamber layout alone. The scheme initially sets chamber pressures for minimum mass flow, determined by the no-outflow criterion. An initial control loop checks lower pressure limits for each chamber on the basis of boundary layer output before proceeding to the stability analysis phase. The most complicated part of the process is the control of chamber pressures on the basis of N-factor output, and the success of the method relies in no small part upon the good qualities of the boundary layer and stability methods used at DERA. Precise resolution of small changes in suction rates is required, as is a smooth response to these changes of the maximum N-factor. The process must also work without any user intervention.

The N-factor control scheme is illustrated in Figure 7 which shows a the development of a typical N-factor curve over a series of discrete suction bands. The effect of each chamber is assessed over two regions: the suction region, *'a'* in the figure, and any gap *'b'* before the start of the next chamber. N-factors are measured relative to the start of the suction-controlled region, labelled *'u'* on the figure this being simplified greatly by the lack of significant upstream-influence of boundary layer control. Consideration is also given to N-factor values at the downstream end of the control region, *'d'* in the figure, since these may place a burden on the following control region if they are close to the N-factor limit. Target N-factors are then derived for the control region, and a revised chamber pressure is prescribed based on these targets. Newton's method is used where possible; interval search where not. In certain circumstances maximum N-factors in a control region may be independent of the chamber pressures and this must be recognised by the control scheme.

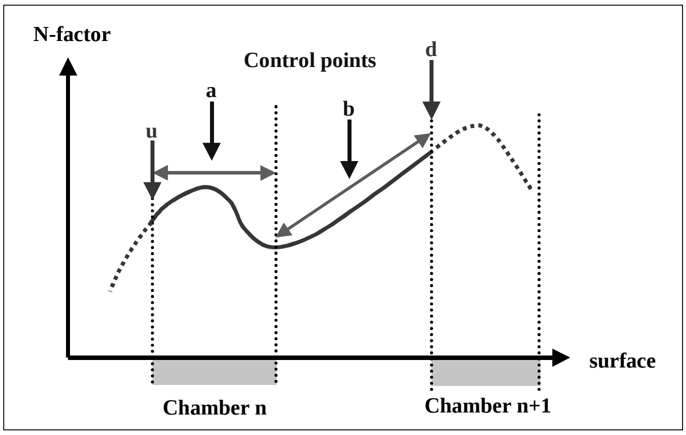

Figure 7: illustration of N-factor control regions.

For multiple chamber arrangements, the upstream chambers are allowed to settle down before the control loop is applied to the downstream chambers.

Notes on Numerical Fluid Mechanics, Vol. 76, P Thiede (ed.), Springer, 2001.
(Proceedings of the CEAS/DragNet European Drag Reduction Conference, Potsdam, June 2000.)

The end result of the process is a chamber pressure specification which observes the N-factor constraints for each control region: usually this represents just one of a number of possible solutions to the control problem (for a fixed chamber layout), but it is easy to adjust chamber pressures manually to investigate other solutions. This usually involves increasing the suction levels over the upstream chambers. The output from the process is chamber pressures and mass flow rates (dependent on the spanwise extent of the chambers) which can be used as the basis for a system design. In the HYLTEC project this approach is being used to investigate HLFC performance issues across all the issues of profile drag, pump power, system weight and cost.

The numerical features of the process are as follows. An interpolation scheme is applied to the basic mean flow specification to include explicitly the chamber start and end points. These are resolved over four intervals of 0.05% chord each. The final distribution of points yields about 100 boundary layer stations for analysis, although the iterative stability calculations are restricted to the currently active control regions, saving unnecessary analysis. Nonetheless at each station the stability of some 400 modes is analysed, and a complete control loop might involve the calculation of between 5000 and 30 000 eigenvalues. The whole process takes from one to four hours on a Pentium 2 PC at 350 MHz depending on the number of chambers involved. Clearly there are enormous opportunities for the replacement of the full stability analysis method with a robust, validated database-type method.

Application of the new process

The opportunities offered to the designer by such a tool are demonstrated by the following examples. The first is a seven chamber layout shown in Figure 8. This can be compared with the manually-designed example presented in Figure 5.

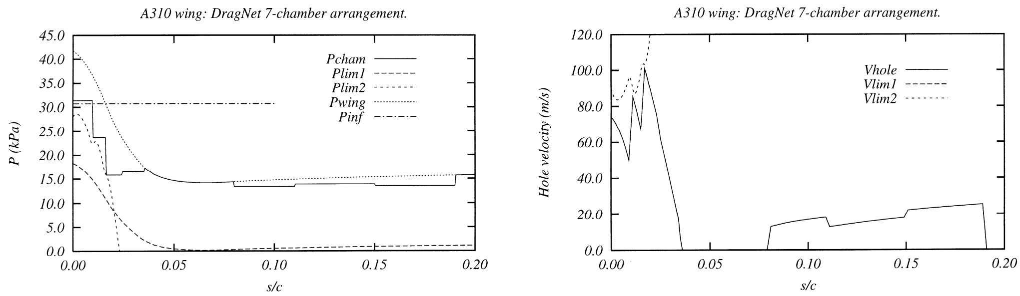

Figure 8 (a) Seven-chamber layout and (b) velocity distribution satisfying the control requirements.

Here the attachment line chamber pressure has been relaxed to achieve a target R_θ along the attachment line: the second and third chambers have been set to give maximum possible suction rates, while the fourth is free to respond to the N-factor distribution. The fifth chamber has been removed, while the sixth has been subdivided into three to introduce some flexibility into the control of the Tollmien-Schlichting modes. Of these three, the middle chamber is at the maximum allowable pressure (with a safety .margin against outflow) while the outer two respond to the N-factor distribution. The saving in mass flow compared to Figure 5 is 19%. The steps leading to this choice of distribution started with simple N-factor control over chambers 2, 3 and 5: the results show that suction over chamber 5 is quite inefficient, and that control is achieved more economically by removing this chamber, which pushes most of the suction into chamber 4 . Shifting suction even further upstream by manually increasing the suction in chambers 2 and 3 reduces the required mass flow rate even further.

Figure 9 illustrates a simplified chamber layout with only three chambers which also satisfies the control requirements. Here the control of crossflow modes is achieved with a single chamber in addition to the one on the attachment line. The middle of the three chambers downstream of the suction peak has been removed. As well as the system simplification, a further 4% reduction (compared to Figure 5) in mass flow is achieved overall (although the TS-control mass flow has increased). Note, however, that the pressure losses have increased.

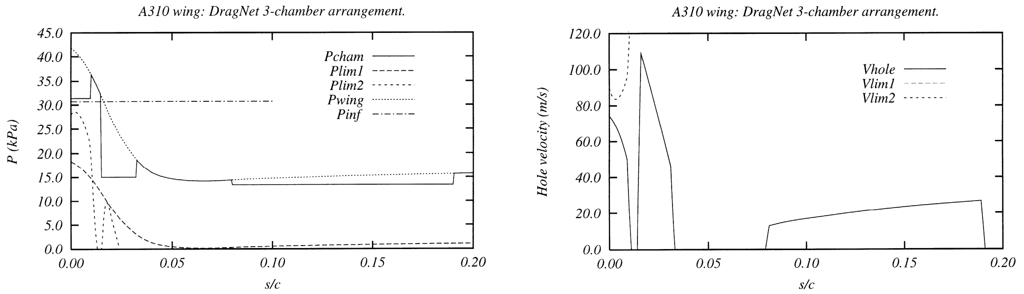

Figure 9 (a) Three-chamber layout and (b) velocity distribution satisfying the control requirements.

The N-factor plots for these two arrangements both look very similar to Figure 4(a) because the chamber pressures have been adjusted iteratively to satisfy the same N-factor control criterion.

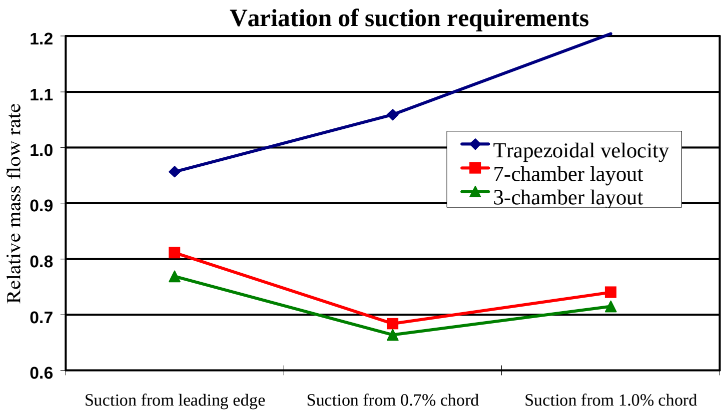

Figure 10: Effect of moving suction away from the leading edge.

The impact of these changes on the system specification, including power requirements, weight and cost, is one the issues being investigated in the HYLTEC project. From the systems point of view the analysis is greatly facilitated by the immediate availability of mass flow and pressure loss information from the aerodynamic design. In all cases it is demonstrable that significant improvements, in terms of reduced mass flow, can be made over the use of a simple trapezoidal transpiration distribution. Any design studies undertaken using a velocity-distribution analysis would be completely obscured by the uncertainties involved in implementing the chamber layout. The present approach allows the implementation to be controlled and compared while the aerodynamic parameters are varied.

Both of the chamber layouts described above feature gaps in the suction distribution which have been introduced on the basis of suction effectiveness. In practical cases there may be a requirement for gaps in the suction distribution to accommodate other systems (e.g. de-icing) near the leading edge. Figure 10 illustrates the effect of moving suction aft from the attachment line for the velocity-distribution, 7-chamber and 3-chamber approaches. Clearly, in mass flow terms, there is a significant benefit in not sucking right at the attachment line (if an alternative contamination avoidance system is used); but there is a point beyond which total suction effort increases for a given configuration. For obvious reasons, the simple velocity-distribution approach fails to capture these effects.

Conclusions and recommendations

An automatic tool has been developed to satisfy N-factor requirements which also allows the designer to constrain chambers en route to an optimised layout. The method relies on the existence of a robust, well-resolved and automatic stability analysis method.

The new approach has highlighted some of the deficiencies of the trapezoidal-velocity-distribution approach. The importance of modelling the control system is perhaps a useful message to those who are developing analytical suction optimisation tools for HLFC design.

A new N-factor control philosophy has been proposed which attempts to balance the technical risk of an HLFC system against commercial gain. The philosophy is based on the likely onset of non-linear behaviour, and the consequent failure of the e^N model. The philosophy must be properly validated and/or modified with further research, particularly in the area of non-local and non-linear analysis of crossflow instability, since it dictates about 50% of the mass flow requirements - at least for the test case presented here.

A review of recent over-suction studies by two different research groups has shown that the two sets of findings differed significantly in terms of important parameters. A hybrid criterion, not yet validated, has been used for the present work: further work in this area is essential to the development of a simple chamber layout and plumbing system. Future work should also focus on the highly swept flow close to the attachment line where the over-suction problem appears to have the greatest impact on high-Reynolds-number HLFC design.

References

1 Atkin C J, Poll D I A. *Correlation between linear stability analysis and crossflow transition near an attachment line*. Transitional Boundary Layers in Aeronautics, Henkes and van Ingen eds., North-Holland, 1996. pp. 155-164.

2 G. Schrauf, J. Perraud, F. Lam, H.W. Stock, D. Vitiello, A. Abbas, *Transition prediction with linear stability theory – lessons learned from the ELFIN F100 flight demonstrator,* 2nd European Forum on Laminar Flow Technology (1996), 8.58-8.71.

3 Preist J, Paluch B. *Design specification and inspection of perforated panels for HLFC suction systems.* Paper 6.3, 2nd European Forum on Laminar Flow Control, Bordeaux (June 1996).

4 Reneaux J, Blanchard A. *The design and testing of an airfoil with hybrid laminar flow control.* 1st European Forum on Laminar Flow Control, Hamburg (March 1992).

5 Ellis J E, Poll D I A. *Laminar and laminarizing boundary layers by suction through perforated plates.* 2nd European Forum on Laminar Flow Technology, Bordeaux (June 1996).